

Supporting Information

Ultrafine NiCo alloy nanoparticles supported on biomass chitin-derived 3D porous carbon substrates as bifunctional catalyst for

ORR and OER

Wenting Liu,^{a, b} Feng Wang,^{*a} Xiaoyu Wu^b and Zhenzhen Wu^b

^a.School of Materials Science and Engineering & Guangxi Key Laboratory of Information Materials, Guilin University of Electronic Technology, Guilin 541004, China.

^b.School of Automobile and Transportation, Shenzhen Polytechnic University, Shenzhen 518055, China.

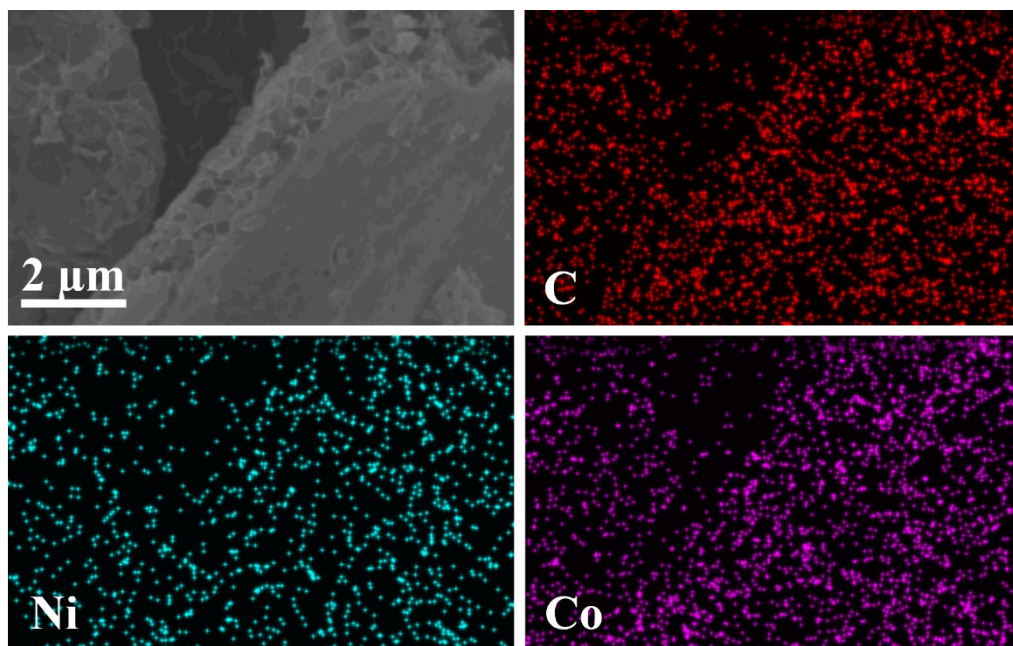


Fig. S1 EDS elements mapping of C, Ni and Co of $\text{Ni}_1\text{Co}_3\text{-K}$

Table. S1The EDS of $\text{Ni}_1\text{Co}_3\text{-K}$

element	atomic number	normalized atomic mass 【%】	atomic 【%】	abs.error【%】 (3 sigma)
Al	13	10.12	30.85	1.33
K	19	4.81	10.12	0.45
Co	27	18.22	25.43	1.11
Ni	28	5.51	7.73	0.58
Pt	78	61.34	25.87	4.74
100.00				

Table. S2 The ICP-MS results of $\text{Ni}_1\text{Co}_3\text{-K}$

Samples	Ni (at.%)	Co (at.%)
$\text{Ni}_1\text{Co}_3\text{-K-1\#}$	26.2526918	73.7473082
$\text{Ni}_1\text{Co}_3\text{-K-2\#}$	26.5249644	73.4750356
Average	26.3888281	73.6111719

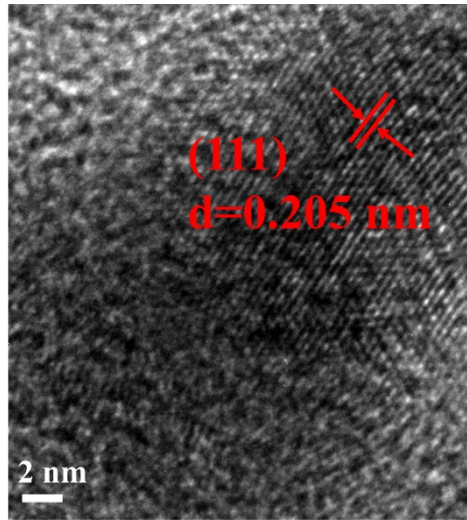


Fig. S2 HRTEM of $\text{Ni}_1\text{Co}_3\text{-K}$ with an aggregated alloy particle

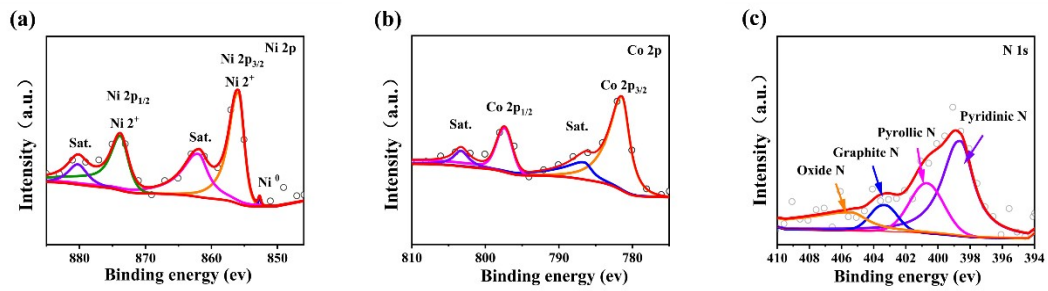


Fig. S3 (a) The deconvoluted XPS spectrum of (a) Ni 2p, (b) Co 2p, (c) N 1s of $\text{Ni}_1\text{Co}_3\text{-K}$

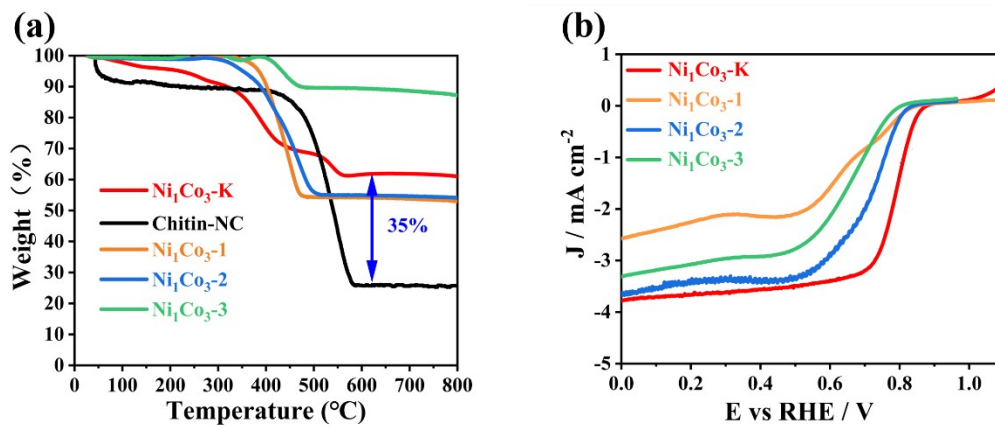


Fig. S4 (a) TG spectra of $\text{Ni}_1\text{Co}_3\text{-1}$, $\text{Ni}_1\text{Co}_3\text{-2}$, $\text{Ni}_1\text{Co}_3\text{-3}$, $\text{Ni}_1\text{Co}_3\text{-K}$ and Chitin-NC, (b)

LSV curves of $\text{Ni}_1\text{Co}_3\text{-1}$, $\text{Ni}_1\text{Co}_3\text{-2}$, $\text{Ni}_1\text{Co}_3\text{-3}$ and $\text{Ni}_1\text{Co}_3\text{-K}$

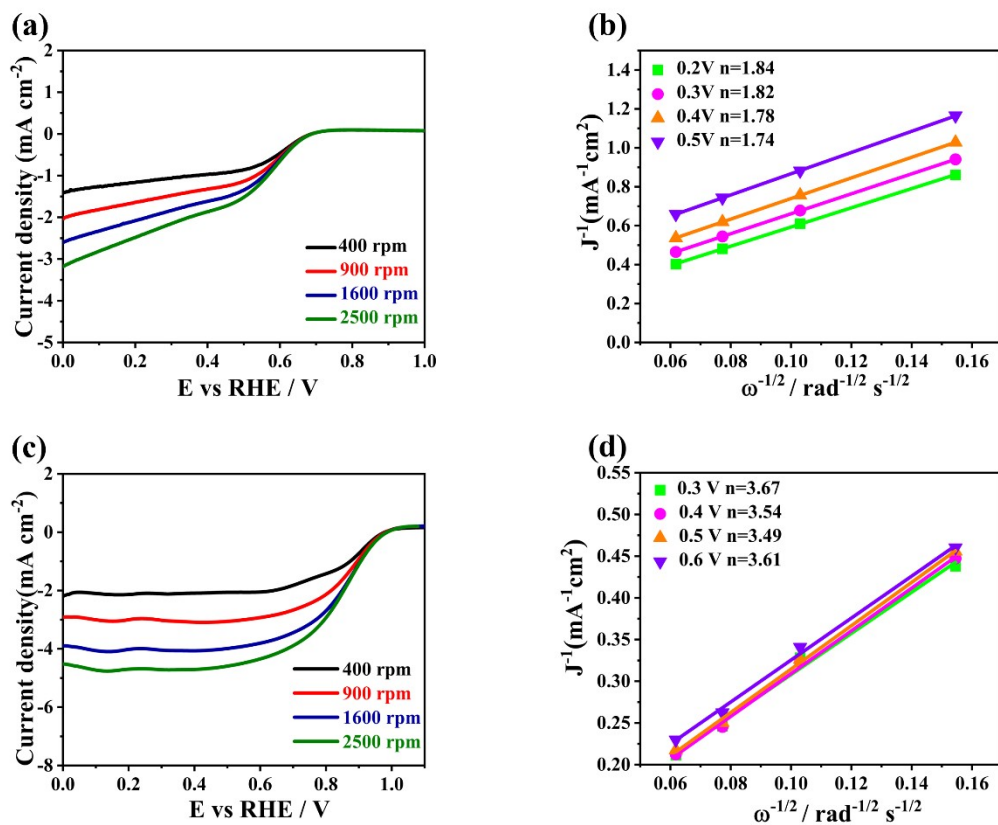


Fig. S5 The LSV curves of the (a) Chitin-NC and (c) Pt/C at different rotation speed with a scanning rate of 10 mV s⁻¹; The corresponding K-L plots of the (b) Chitin-NC and (d) Pt/C at different electrode potentials

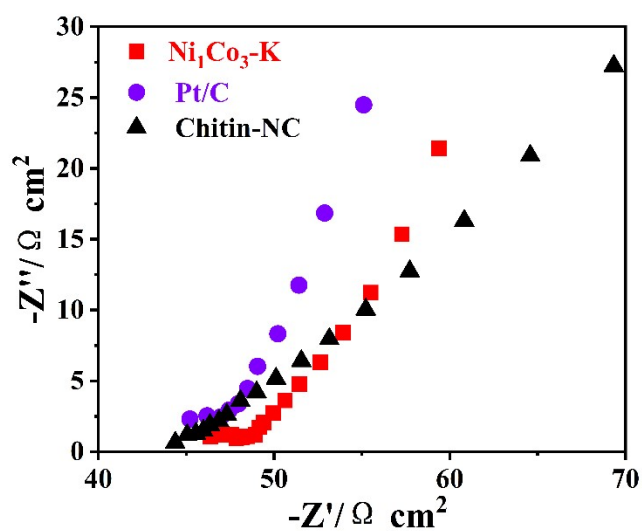


Fig. S6 The Nyquist plot of the catalysts towards ORR

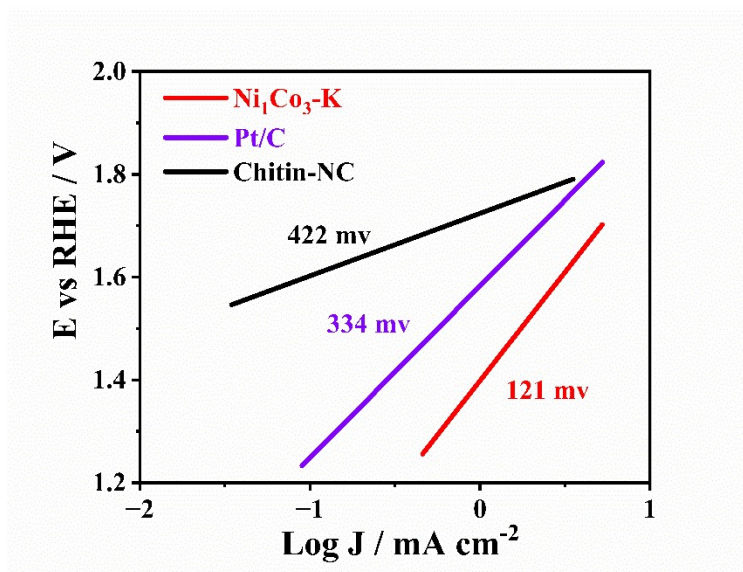


Fig. S7 Tafel plots of Ni₁Co₃-K, Chitin-NC and Pt/C

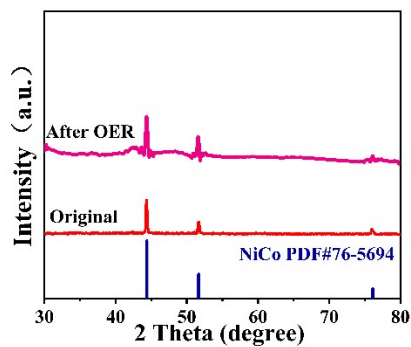


Fig. S8 The XRD of Ni₁Co₃-K before and after OER stability test

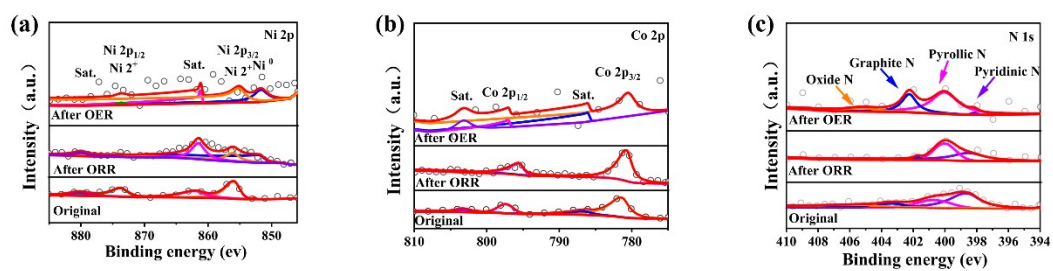


Fig. S9 The deconvoluted XPS spectrum of (a) Ni 2p, (b) Co 2p, (c) N 1s of Ni₁Co₃-K before and after ORR and OER stability tests

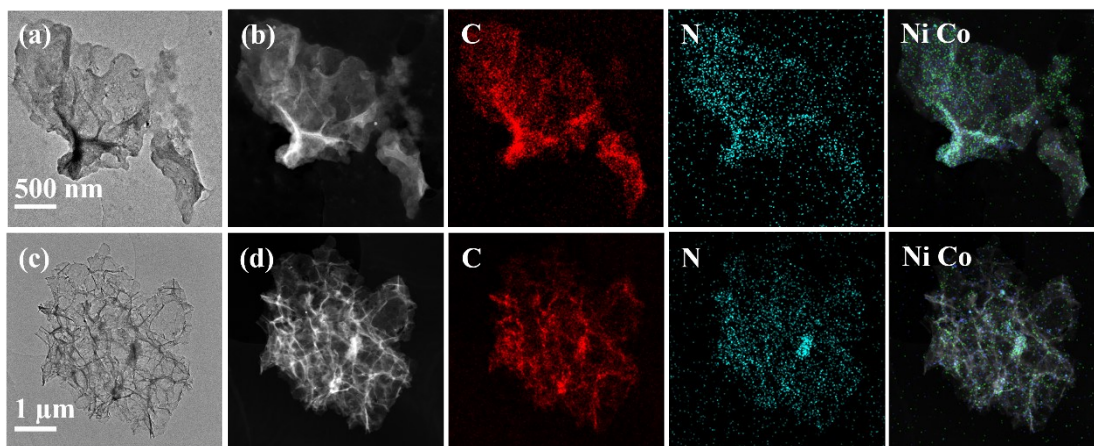


Fig. S10 The HAADF-STEM and relevant EDS elements mappings of $\text{Ni}_1\text{Co}_3\text{-K}$ after stability test (a, b) OER, (c, d) ORR

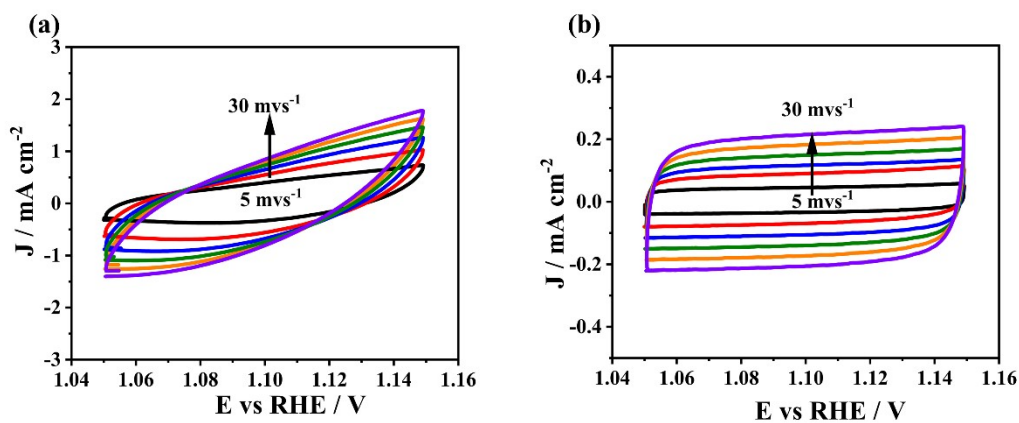


Fig. S11 The CV curves recorded in non-Faradaic region with scan rate of 5, 10, 15, 20, 25, 30 m V s^{-1} of $\text{Ni}_1\text{Co}_3\text{-K}$ (a) and Pt/C

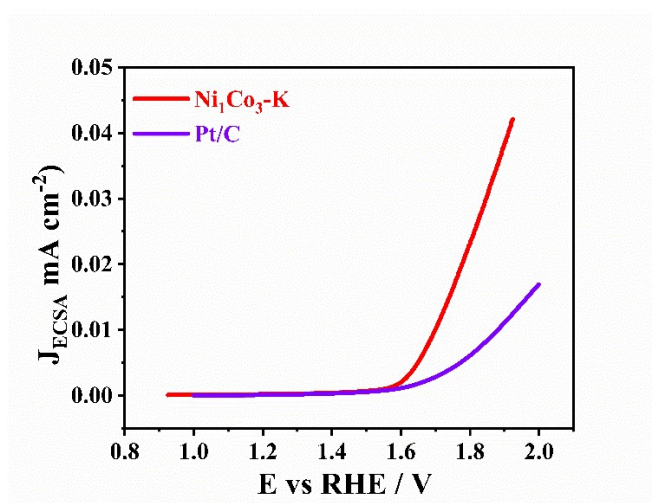


Fig. S12 The ECSA normalized-LSV curves of $\text{Ni}_1\text{Co}_3\text{-K}$ and Pt/C

Table S3 Comparison with other reported bifunctional catalysts

Electrocatalysts	Electrolyte	$E_{1/2}$	ΔE	Reference
Ni ₁ Co ₃ -K	0.1M KOH	0.78	0.85	This work
Co-ADC	0.5M KOH	0.78	0.89	[1]
NdBaCo _{1.8} Fe _{0.2} O ₅	0.1M KOH(ORR)& 1M KOH(OER)	0.73	0.95	[2]
Mn-Co ₃ O ₄	0.1M KOH	0.69	1.11	[3]
Fe/Ni-DA-CNFs	0.1M KOH	0.79	0.88	[4]
FeMnO ₃ /CNT	0.1M KOH	0.74	0.89	[5]
Cu _{0.2} -NiOSC	0.1M KOH	0.78	0.93	[6]
CoO@Co-N-C	0.1M KOH	0.79	0.86	[7]
NiCo ₂ O ₄ -GO/C	0.1M KOH(ORR)& 1M KOH(OER)	0.79	0.88	[8]
KB@Co-C ₃ N ₄	0.5MNH ₄ Cl	0.723	1.05	[9]

Reference

- [1] Audeves–Audeves Y, Arredondo–Espínola A, Nava O, et al. High activity of cobalt-atomically dispersed catalyst on mesoporous carbon for rechargeable Zn-air batteries via effective removal of the hard template [J]. *Micropor Mesopor Mat*, 2025, 381 113359.
- [2] Ozgur C, Erdil T, Geyikci U, et al. B-Site Doping Boosts the OER and ORR Performance of Double Perovskite Oxide as Air Cathode for Zinc-Air Batteries [J]. *Chemphyschem*, 2024, 25 (22): e202400531.
- [3] Shui Z Y, Yu S L, Lu W, et al. Bifunctional Electrocatalysts of Mn-doped Co₃O₄ for Oxygen Reduction and Oxygen Evolution Reactions in Alkaline Medium [J]. *Acta Chim Sinica*, 2024, 82 (10): 1039-1049.
- [4] Zheng Y, Zhu G, Li G, et al. Fe, Ni doped carbon nanofibers as dual functional electrocatalyst prepared by in-situ grown SiO₂-protected in nanoconfinement [J]. *Diamond and Related Materials*, 2024, 142 110761.
- [5] Thomas A A, Eledath A N, Niranjana J S, et al. FeMnO₃/CNT as a synergistic bifunctional electrocatalyst for oxygen reduction and oxygen evolution reactions in alkaline medium [J]. *Materials Chemistry and Physics*, 2024, 324 129695.
- [6] Zhang J, Zhuge X, Liu T, et al. Copper-doped nickel oxide supported on carbon black for highly active oxygen reduction/evolution electrocatalysis [J]. *Materials Today Communications*, 2024, 38 108335.
- [7] Gan L, Han L, Liu J, et al. In-situ grafting of CoO nanosheets onto hollow CoNC matrix for an enhanced bifunctional oxygen electrocatalyst [J]. *Journal of Electroanalytical Chemistry*, 2024, 968 118503.
- [8] Fu L X, Yao Y F, Ma J L, et al. Nanoflower-like NiCo₂O₄ Composite Graphene Oxide as a Bifunctional Catalyst for Zinc-Air Battery Cathode [J]. *Langmuir*, 2024, 40

(13): 6990-7000.

- [9] Wu W-F, Fan J-G, Zhao Z-H, et al. Wonton-structured KB@Co-C₃N₄ as a highly active and stable oxygen catalyst in neutral electrolyte for Zinc-air battery [J]. Chinese J Catal, 2024, 60 178-189.